Molecular Dynamics Computer Simulation of Polyisoprene Local Dynamics in Dilute Toluene Solution

Neil E. Moe and M. D. Ediger*

Department of Chemistry, University of Wisconsin, Madison, Wisconsin 53706

Received August 29, 1994; Revised Manuscript Received January 19, 1995[⊗]

ABSTRACT: Fully atomistic molecular dynamics computer simulations have been performed on a polyisoprene chain of 35 repeat units in a solution of 207 toluene molecules. Simulated orientation correlation functions of polymer C−H vectors compare favorably with ^{13}C NMR experiments. In particular, the ordering of the different correlation times is as expected, and their absolute values agree with experiment within a factor of 2. Also in good agreement with experiment, backbone C−H correlation functions were found to be nearly exponential after a very fast small-amplitude decay. The simulation trajectories have been analyzed to examine the changes in atomic positions and torsional coordinates which accompany conformational transitions. Adjustments in these degrees of freedom are found to be localized to 1−2 repeat units in polyisoprene, in good agreement with the results of previous Brownian dynamics simulations. Cooperative pairs of conformational transitions account for less than half of all transitions if coupling up to second neighbors is considered. About two-thirds of all transitions occur in cooperative pairs if coupling up to ninth neighbors is considered.

I. Introduction

Local segmental dynamics play a significant role in determining bulk polymer properties such as the glass transition temperature T_g and the temperature dependence of the viscosity. An illustration of this is provided by recent NMR experiments which measured the dynamics of individual C−H vectors in polymers over a wide range of time scales.[1,2] These very local motions have a temperature dependence very similar to that of the α relaxation as determined by mechanical measurements. Thus local dynamics on the scale of a few repeat units are intimately connected to the glass transition.

Even the most powerful experiments cannot answer all of the interesting and important questions about local polymer dynamics. For example, what types of cooperative motion allow conformational transitions to take place in the middle of a polymer chain? Over what length scales are motions cooperative? What role does the potential energy surface play in local polymer dynamics? Computer simulations provide a means of directly examining the detailed mechanisms of local polymer dynamics.

We report here molecular dynamics simulations of a polyisoprene chain in a dilute toluene solution. We selected a solution simulation since local dynamics in solution are likely to be relevant to dynamics in the bulk and easier to understand than bulk dynamics. While atomistic molecular dynamics simulations have been previously used to study conformational dynamics in a number of bulk polymer systems,[3−6] the present study is one of the first on a polymer/solvent system.[7] Polyisoprene was chosen for these simulations for three reasons. First, polyisoprene is dynamically very flexible; i.e., conditions can be chosen so that the local dynamics occur on a sub-100 ps time scale at experimental temperatures. This allows a reasonable description of the local dynamics in the short time window available in molecular dynamics simulations. Second, being an important industrial polymer, there are extensive experimental data on the local dynamics of polyisoprene in dilute solution[8,9] and in bulk.[10−12] This allows a test of the accuracy of the simulation. Third, Adolf and Ediger have previously reported Brownian dynamics simulations on a closely related system.[13]

A previous Brownian dynamics simulation on polyisoprene in solution reported several important conclusions.[13] Distortions in atomic positions accompanying conformational transitions were found to be very localized, involving only about one repeat unit. Cooperative transition pairs (through second neighbors) accounted for less than half of all transitions. Librational motions on the scale of a few ps were found to play a significant role in the decay of the orientation autocorrelation function for C−H vectors. Because of the approximations involved in the Brownian dynamics study, the above conclusions were regarded as somewhat tentative.

The present study confirms all of the above results of the Brownian dynamics simulations on polyisoprene. In addition, solvent and polymer dynamics in these simulations correctly reproduce all of the qualitative features of the experimental results for the polyisoprene/toluene system. Absolute correlation times from the simulation agree with experiment to within a factor of 2. The agreement between experiment and simulation, and between Brownian and molecular dynamics, makes us reasonably confident that the main features seen in these simulations are realistic.

II. Simulation and Description

Molecular dynamics simulations solve Newton's equation of motion

$$\vec{F}_i = m_i \vec{a}_i \tag{1}$$

for a collection of particles. The force $\vec{F}_i$ on an individual particle is determined by the gradient of the potential energy at its location. If the initial positions and velocities of each particle are specified, eq 1 can be integrated iteratively to generate new positions and velocities as a function of time. This trajectory can then be processed to extract static and dynamic properties of interest.

The molecular dynamics simulations reported in this paper were performed using Biosym's *Amorphous Cell* and *Discover* programs.[14] The model system was fully atomistic. We used Biosym's CFF91 force field[15] to

[⊗] Abstract published in *Advance ACS Abstracts,* March 1, 1995.

0024-9297/95/2228-2329$09.00/0

define the potential energy for our system.[16] In general, every atom center interacts with every other in the system through either nonbonded or bonded potential terms. The nonbonded potentials are a sum of Lennard-Jones-like interactions (6−9) and Coulombic partial charge terms. The bonded potential terms include bond bending, bond stretching, torsions, and cross-terms which couple these. The parameters in the force field are designed to be transferable; no attempt was made to tailor the force field to our particular system.

The main simulation presented here is a nanosecond trajectory of a 35-mer of polyisoprene and 207 toluene molecules. The polyisoprene used was 100% *cis*- and had all head-to-tail linkages; its structure is shown below:

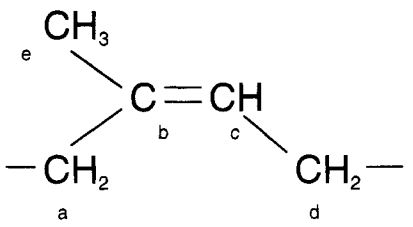

NMR measurements on polymer solutions indicate that the local polymer dynamics are independent of solution concentration below about 15% polymer by mass.[17] Our simulated system is 11.1% polymer by mass and thus the simulated dynamics should be representative of local dynamics at infinite dilution. Experiments on a number of different polymers indicate that the local dynamics of a polyisoprene 35-mer should be essentially the same as those of a high molecular weight polymer.[17] In particular, solution NMR measurements on polyethylene oligomers with the same number of backbone carbon atoms indicate that the limiting high molecular weight behavior has been attained.[18] A nanosecond trajectory for this system of 3562 atoms took 50 days of CPU time on an IBM RS6000/325.

Although our main interest in this simulation was the local dynamics of polyisoprene, we performed a number of simulations on neat toluene in order to ensure that our solvent bath had realistic dynamics. These simulations were also used to establish various simulation parameters. We will present the results leading to the choice of simulation parameters here and reserve a more complete comparison with experiment until section III. Integration time steps of 1.0 and 0.5 fs were found to yield identical results, so the larger time step was used. Potential cutoff distances of 8.0 and 10.0 Å likewise yielded indistinguishable results. A truncation of the potential energy was applied at 8.0 Å using a sharp cutoff rather than using a polynomial switching function. Simulations of liquid argon which we performed indicated that using a sharp cutoff reproduced the large-cutoff dynamics more faithfully than did a switching function. Simulation cells of 98 and 215 toluene molecules were analyzed in order to identify system size effects. The dynamics of the larger system were somewhat faster than those of the smaller; it is not known whether a still larger system would yield even faster dynamics. Since the dynamics of the larger box compared favorably with experiments, we concluded that it would provide a suitable environment for simulating the polyisoprene chain.

All simulations were carried out at 298 K and used the NPT ensemble (the density is allowed to fluctuate) unless stated otherwise. All reported pressures include the long-range correction necessary due to the potential energy truncation. Cubic periodic boundary conditions were used.

Table 1. Polyisoprene/Toluene Simulations[a]

	constant	length, ps	$\langle\rho\rangle$, g/cm^3	$\langle r^2\rangle^{0.5}$, Å	$\langle r_g^2\rangle^{0.5}$, Å
run 1	*P*	990	0.820	25.7	13.7
			(0.003)	(4.5)	(1.7)
run 2	*V*	120	0.860	31.0	15.3
				(3.8)	(0.2)
run 3	*P*	120	0.827	52.6	15.3
			(0.001)	(2.3)	(0.2)
run 4	*P*	120	0.826	37.0	16.8
			(0.004)	(2.3)	(1.0)
run 5	*P*	120	0.829	12.6	9.4
			(0.002)	(1.3)	(0.2)

[a] Parentheses indicate standard deviations of 30 ps block averages.

Neat Toluene. The initial toluene configurations were generated at bulk density (0.860 g/cm^3) using *Amorphous Cell*. After 100 steps of steepest descents minimization, 50−100 ps of molecular dynamics were performed to equilibrate the system. During equilibration, the pressure was gradually lowered from 2000 to 1 atm; the high initial pressure kept the system from expanding significantly due to unfavorable interactions. After equilibration, 120 ps trajectories were performed and various static and dynamic quantities were calculated. The densities of the systems showed no systematic trends during this period.

Main Solution Trajectory (Run 1). Several different structures with 35 isoprene units were initially generated in a vacuum using random torsional angles. From experimental results on high molecular weight polyisoprene chains,[19] we estimate that isoprene 35-mers have end-to-end distance $\langle r^2\rangle^{0.5} = 40$ Å and radius of gyration $\langle r_g^2\rangle^{0.5} = 16$ Å.[20] Hence we chose a structure which had an initial end-to-end distance of about 40 Å; visually this structure appeared open without any regions of high segment density. One hundred steps of steepest descents minimization and 1 ps of dynamics were first performed. The 35-mer was then added to an already equilibrated toluene box, eliminating any toluene molecules which overlapped with the polymer. At this stage, the cell density was about 0.6 g/cm^3. Minimization (100 steps) and dynamics (1 ps) were then performed at constant volume. Constant-pressure dynamics was used to generate the rest of the trajectory. A total of 250 ps was allowed for equilibration. The simulation pressure was started at 1600 atm and gradually lowered to 100 atm in the first 70 ps, then held constant at 100 atm for 150 ps, and then lowered to 1 atm from the final 30 ps. Various static and dynamic properties were calculated during an additional 990 ps trajectory at 1 atm. The density displayed no systematic trends over this time interval. Some characteristics of the solution trajectories are summarized in Table 1.

Constant-Volume Trajectory (Run 2). Most of our simulations of polyisoprene in toluene were performed at a constant pressure of 1 atm. Although the experimental density of an 11% polyisoprene/toluene solution has not to our knowledge been reported, the simulation densities are likely too low. The actual density is probably close to the neat solvent density. This discrepancy is presumably due to a deficiency in the force field. The low value of the density in the neat toluene simulation (see Table 2) is consistent with this explanation.

Table 2. Toluene Dynamics

	expt (neat toluene)	98 toluene[a]	215 toluene[a]	207 toluene/PI[a,b]
rotation (τ_c/ps)				
o	2.1 ± 0.2[c]	2.0 (0.1)	1.7 (0.1)	1.62(0.02)
m	2.1 ± 0.2[c]	2.0 (0.1)	1.7 (0.1)	1.60(0.02)
p	2.6 ± 0.3[c]	2.8 (0.1)	2.4 (0.1)	2.27(0.05)
translation (D × 10^9/m^2 s^{-1})	2.3 ± 0.3[d]	1.2 (0.2)	1.7 (0.2)	1.83(0.07)
density (g/cm^3)	0.860	0.844 (0.003)	0.833 (0.002)	0.820 (0.001)

[a] Parentheses indicate 90% confidence intervals. [b] Run 1. [c] References 22, 23, and 25. Errors indicate range of reported results including uncertainty in the coupling constants. [d] References 24 and 26.

To determine the effect of simulating our system at a more realistic density, we took a frame from the middle of run 1 and restarted dynamics at high pressure. When the system reached the experimental solvent density, 120 ps of constant-volume molecular dynamics were performed and statistics were collected. The pressure (around 775 atm) showed no systematic trends over this time interval. Because the chain configuration in this run was essentially identical to that of run 1, this procedure allowed us to isolate the effect of density on the local polymer dynamics.

Additional Solution Trajectories (Runs 3–5). Experimental results on higher molecular weight chains indicate that the longest relaxation time for a 35-mer of polyisoprene in a dilute toluene solution is 5–10 ns.[21] Thus a 1 ns trajectory is not nearly long enough to allow one initial polymer configuration to completely explore phase space. We performed several shorter simulations to compare with run 1 in order to estimate the effect of initial configuration on the simulated dynamics. We generated 10 additional polymer structures as before and chose three to investigate further. Two had open and extended conformations similar to run 1, while one was much more compact ($\langle r^2\rangle^{0.5}$ values are given in Table 1). These structures were added to toluene boxes and treated identically to the main polymer until the equilibration step. Only 70 ps of equilibration was allowed, during which the pressure was taken from 1600 to 1 atm. This was followed by a 120 ps trajectory during which static and dynamic properties were calculated. Again, the densities displayed no systematic trends over these time intervals, although the average density in each case was slightly higher than in run 1 (see Table 1).

Torsion Populations. The polyisoprene backbone has three different types of carbon–carbon single bonds per repeat unit. This implies three different torsions, which we refer to as ab, cd, and da (see structure above). Figure 1 shows symmetrized population distributions for these three torsions as calculated from run 1. The effective potentials (a potential of mean force) for each of the three torsions can be inferred from the figure. The effective potential for torsion da has three wells while torsions ab and cd are 2-fold, torsion cd being more "loose" (i.e., lower barrier). In constructing Figure 1, $\phi = 0$ for torsions ab and cd was defined to place all the carbon atoms of the polymer in the same plane, as in the structure above. For torsion da, the *trans* state was defined to be $\phi = 180$. The populations used to construct Figure 1 were not quite symmetric, presumably due to the finite simulation time.

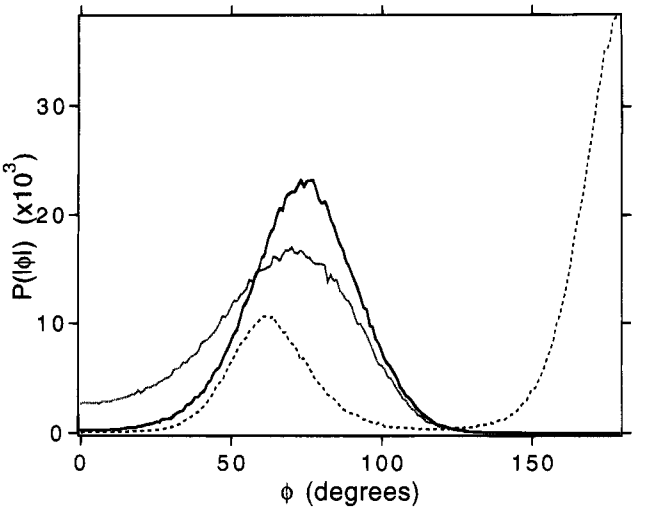

Figure 1. Symmetrized population distributions for torsions ab (thick line), cd (thin line), and da (- - -) from run 1.

III. Comparison with Experiments

In this section we compare the dynamics from our simulations to experimental results. These comparisons indicate that the dynamics of both the solvent and the polymer are reproduced in our simulation within a factor of 2. The microscopic picture of local dynamics which emerges from these simulations is discussed in section V.

Solvent Properties. Simulated toluene was compared with NMR measurements[22–26] of the translational diffusion coefficient D and the rotation times τ_c for the three C–H bond vectors in the aromatic ring. The diffusion coefficient was calculated from the long-time slope of a plot of the mean squared displacement of toluene centers of mass vs time using the relationship

$$\langle r^2\rangle = 6Dt \tag{2}$$

The C–H vector reorientation times depend upon the decay of the P_2 orientation autocorrelation function:

$$CF(t) = \langle P_2(\hat{x}(0)\cdot\hat{x}(t))\rangle = \langle 3\cos^2\theta(t) - 1\rangle/2 \tag{3}$$

Here P_2 is the second Legendre polynomial, $\hat{x}(t)$ is a unit vector in the direction of a particular C–H bond vector at time t, and $\theta(t)$ is the change in the vector orientation between time t and time 0. The orientational correlation time τ_c is the time integral of the correlation function:

$$\tau_c = \int_0^\infty CF(t)\,dt \tag{4}$$

Qualitatively, rapidly decaying correlation functions result in small τ_cs and imply fast dynamics. For toluene, we integrated $CF(t)$ for the *ortho*, *meta*, and *para* C–H bond vectors in order to obtain τ_c values.

Table 2 shows a comparison between the toluene dynamics observed in our simulations and experimental results. In all cases, the dynamics of the larger neat toluene system are within 25% of the experimental numbers, although translation and rotation are too slow and too fast, respectively. The toluene dynamics are basically unaffected by the addition of polymer, consistent with NMR experiments[25] performed under comparable conditions.

We have also compared static properties of our simulated toluene to experimental results. As shown

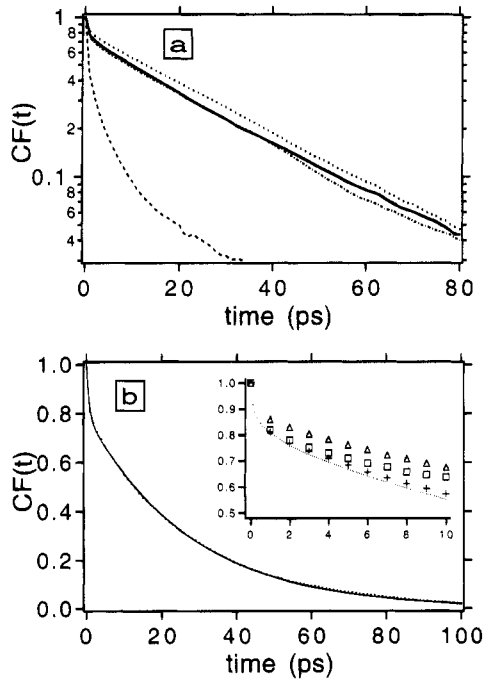

Figure 2. (a) Semilogarithmic plot of P_2 orientation autocorrelation functions for polyisoprene C−H bond vectors a (—), c (···), d (-··-), and e (- - -) from run 1. The long components of the correlation functions for vectors a, c, and d are very close to exponential, in good agreement with experiment. (b) Correlation function for vector c from run 1 (···) with the fit to eq 5 (—) showing decay on two well-separated time scales. The inset shows the initial correlation function decays for C−H bond vector c from run 1 (···), run 2 (+), run 3 (□), and run 4 (Δ).

in Table 2, the simulation density is about 3% too low at 1 atm. While no experimental pair correlation function $g(r)$ data is available to our knowledge, our calculated $g(r)$ was quite similar to that calculated for benzene by Linse.[27] We observed a slight tendency for the rings in toluene neighbors to align perpendicular rather than parallel in the liquid state.

Polymer Properties. Experimental measurements of the local dynamics of polyisoprene in a dilute solution of toluene are reported in refs 8 and 28. In particular, NMR measurements of the orientation correlation times τ_c (see eqs 3 and 4) of the four distinct C−H bond vectors are available for comparison. We designate these bond vectors by the carbon atom to which they are attached: a, c, d, and e in the structure in section II. Figure 2a shows these correlation functions from run 1 in a semilogarithmic format. The five repeat units at each end of the simulated polyisoprene chain were excluded from the calculations to avoid end effects.

Both the shapes of the correlation functions and the time scale for their decays are of interest. Comparisons between the simulation results and experiment are facilitated by fitting the simulated correlation functions to the following analytical function:

$$CF(t) = a \exp(-t/\tau_1) + (1 - a) \exp[-(t/\tau_2)^\beta] \quad (5)$$

with $\tau_1 < \tau_2$. We selected eq 5 because it is a simple function which provides an excellent fit to the simulated correlation functions for C−H vectors in the polymer backbone (a, c, and d). The quality of the fits is illustrated for C−H vector c in Figure 2b. Our simulated correlation functions, in contrast to those obtained from Brownian dynamics simulations, could not be adequately fit to a correlation function with a single time constant (such as the second half of eq 5). We emphasize that eq 5 has not been derived from a microscopic model of local polymer dynamics. We believe that the conclusions which we reach using eq 5 could be reached using any function which provides a good fit to the simulated correlation functions.

Table 3. Fitting Parameters for Run 1 (Eq 5)

C−H vector	a	τ_1/ps	τ_2/ps	β	τ_c/ps
a	0.186	0.250	22.6	0.835	20.3
c	0.196	0.621	27.3	0.986	22.2
d	0.298	0.722	26.5	1.02	18.6

Table 4. Polyisoprene Correlation Times (τ_c/ps)

C−H vector	run 1[a]	run 2	run 3	run 4	expt[b]
a	20.3 (4.4)	30	55	49	35[c]
c	22.2 (4.5)	32	60	56	45[c]
d	18.6 (3.5)	26	52	39	31[c]
e	3.7 (0.3)	4	7	8	7.4[d]

[a] Parentheses indicate standard deviation of correlation times calculated from 120 ps sections of run 1. [b] Approximately 10% error. [c] Reference 9, using revised coupling constants from ref 8. [d] Reference 28.

For run 1, the first 150 ps of the correlation functions for vectors a, c, and d were fit to eq 5. The resulting fitting parameters are shown in Table 3. Analytical integration to $t = \infty$ provided the correlation times. Direct numerical integration yielded very similar values. The orientational relaxation of vector e (the methyl C−H vector) is much faster than the others because it is not attached directly to the polymer backbone and rotates almost freely about the "be" bond. The correlation function for vector e was not fit well by eq 5. This correlation time was calculated by numerical integration.

The statistical noise in the correlation functions from the shorter runs was greater so a slightly different procedure was used. We fit the first 60 ps of the correlation functions from runs 2−4 to eq 5 with the β values fixed at the values obtained from run 1 (given in Table 3). Equation 5 was then integrated analytically to $t = \infty$ to find τ_c.

Table 4 indicates that the τ_c values calculated from run 1 are faster than the experimental results, but agree within a factor of 2. The τ_c values for the different C−H bond vectors are in the expected order; i.e., e is faster than d is faster than a is faster than c. Overall, we consider the agreement between simulation and experiment to be reasonable. The differences may be due to system size, force field deficiencies, and/or short simulation time.

Effect of Density and Initial Configuration. Runs 2−5 were performed to determine the effect of density and initial configuration on the observed dynamics. These runs had shorter equilibration times and trajectory lengths than run 1. As a result, conclusions drawn from these runs are necessarily somewhat imprecise. As shown in Table 4, runs 2−4 had correlation times within a factor of 3 of those from run 1 and within a factor of 2 of the experimental values. We interpret the comparison between runs 1 and 2 to indicate that qualitative conclusions about local dynamics based on run 1 would probably also be valid for a long run at the experimental density. We interpret the comparison between runs 1, 3, and 4 to indicate that different reasonable initial configurations will not produce tremendously different correlation times. The mechanism of local polymer dynamics in these three runs appears

to be the same (see inset to Figure 6). The factor of 3 differences observed may be typical when comparing ns or sub-ns trajectories using different reasonable starting configurations in solution.

Run 5 was unusual in several respects. The chain was very compact compared to our estimate of average chain dimensions. In addition, the overall potential energy was much higher than the other four runs (by about 2 kT per atom). Thus we will not consider run 5 further except to comment that the dynamics from this run were about 10 times slower than those of run 1.

IV. Correlation Function Shapes

The shape of the orientation correlation function provides some information about the mechanism of local polymer motions. The correlation functions for C−H vectors a, c, and d in Figure 2a show a very rapid initial drop followed by a much slower decay, qualitatively indicating that a C−H vector can lose its orientation two ways. As shown in section V, librational motions near the bottom of a potential well occur on very fast time scales and cause partial loss of orientation. Relatively infrequent conformational transitions from one potential energy minimum to another result in the slower decay. Brownian dynamics simulations on polyisoprene did not show two distinct time scales for the correlation function decays.[13] Reference 13 suggested that this was due to unrealistic damping of very high frequency motions by the high-friction Langevin equation.

Since we are mainly interested in the mechanism of conformational transitions, we will further consider the nature of the slow part of the correlation function decay. As the semilogarithmic plot in Figure 2a shows, the correlation functions for the C−H bond vectors attached to the polymer backbone decay nearly exponentially after about 1 ps. Fits to eq 5 provide a more quantitative test of this observation. The βs for the three backbone C−H bond vectors a, c, and d are very close to unity (see Table 3), where $\beta = 1$ means a simple exponential. The fits to eq 5 are very good for $t > 1$ ps; a single exponential describes the short-time decay of $CF(t)$ less well.

The observation that the $CF(t)$ for the backbone C−H bond vectors of polyisoprene in solution decays on two widely separated time scales is consistent with NMR experiments performed by Gisser *et al.*[8] They determined that the slow component was very close to a single exponential, in good agreement with our simulation. They estimated that the fast component accounted for around 45% of the correlation function decay. This result is somewhat larger than the 20−30% which we determined from fits to eq 5 (the values of the parameter a are shown in Table 3). Nevertheless, the experiments and simulations on polyisoprene in solution agree that very fast motions result in a significant initial drop in $CF(t)$. Experiments on bulk polyisoprene have been interpreted similarly.[29]

There are a number of indications in the literature that motions on a third and even longer time scale contribute to the correlation function decay.[30] Evidence for a very low amplitude long-time tail was seen in the NMR experiments[9] of Glowinkowski *et al.* and in computer simulations by Weber and Helfand[31] and Smith *et al.*[32] Backbone C−H vectors cannot completely randomize their orientations until the entire chain loses memory of its starting configuration. The time scale of this long decay is thus molecular weight dependent and typically at least several orders of magnitude slower than the time scale for conformational changes. Obviously this component is not seen in Figure 2 and does not contribute to the correlation times in Table 4. Fortunately, any contribution from this component is also excluded from τ_c values calculated from the NMR experiment.[9,30] Thus the comparison between experiment and simulation in Table 4 is legitimate.

Comparison to Theoretical Models. We wish to comment briefly on the correlation function shapes shown in Figure 2 in relation to the prediction of various theoretical models. We consider here the models of Hall and Helfand,[33,34] Jones and Stockmayer,[35] and Bendler and Yaris.[36] For most values of the adjustable parameters in these functions, the predicted correlation function shapes are quite nonexponential. Since none of these models consider librational motions,[37] a fair comparison to our simulated correlation functions involves only the longer component shown in Figure 2. Thus it is striking that this component decays very nearly as a single exponential.

Can any of these theoretical models rationalize a single-exponential decay? The Hall−Helfand model predicts a single-exponential decay only when there are no cooperative transition pairs. We will show below that this is not the case. The Bendler−Yaris model predicts a single-exponential decay only when the length scale for dynamic correlations along the chain backbone is equal to the size of the smallest flexible unit. Calculations at the end of section V indicate that this is not the case. The Jones−Stockmayer model cannot produce a single-exponential decay for any parameters considered in ref 35.

One might object that it is unfair to expect a conceptual molecular model to explain the details of a fully atomistic simulation. Indeed, these models do not explicitly account for the chemical structure of the polymer repeat unit. Yet these same models have been used to fit experimental data with the resulting parameters being interpreted as literally as in the previous paragraph. Our point is simply that parameters which are obtained by fitting conceptual molecular models to experiments or simulations need to be interpreted with caution.

V. Microscopic View of Local Polymer Dynamics

In this section we use four different methods to characterize the mechanism of local dynamics in our simulated polyisoprene chains. These methods provide information which is not directly accessible from experiments. The previous two sections indicate that all qualitative features of the experimental results for polyisoprene local dynamics in solution are reproduced by our simulation. Absolute time scales for motions in the simulation are correct within a factor of 2. Given that the simulation is reasonably realistic in predicting experimental observables, we are optimistic that the microscopic features discussed in this section are also reasonably realistic.

Time Evolution of Torsional Coordinates. Figure 3 shows the probability P of observing an angular change $|\Delta\phi|$ during various time intervals for the 3-fold torsion da.[13] Within 0.3 ps, many torsions have already adjusted by 10−30°. This feature of the torsional angle distribution changes little as time evolves. At much longer times, new peaks centered at 120 and 240° grow in, indicating transitions to other conformational states.

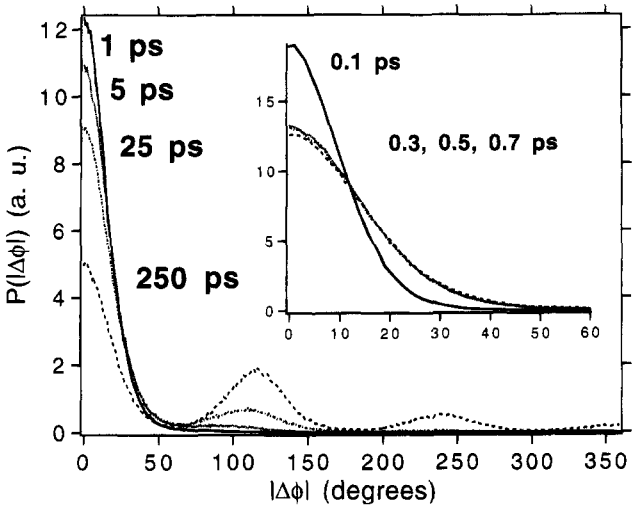

Figure 3. Probability of angular change $|\Delta\phi|$ of torsion da in various time intervals. Each time step in the trajectory was used as a starting time in calculating this quantity. The inset uses smaller time intervals. Librational motions in the bottom of potential wells equilibrate in about 0.3 ps, while conformational transitions occur at much longer times.

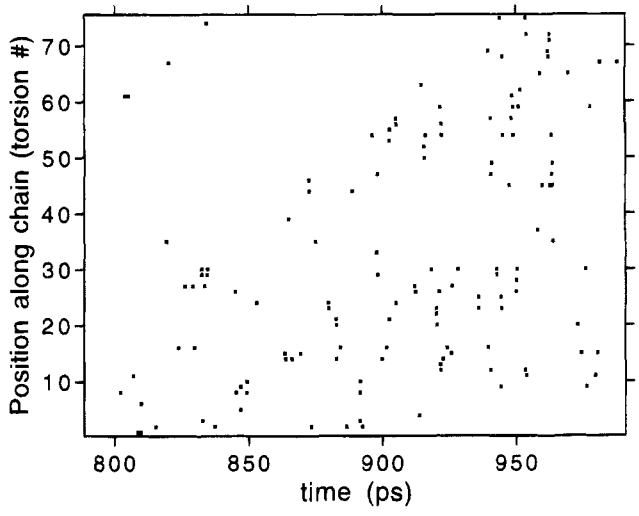

Figure 4. Map showing the positions in space and time of conformational transitions from the last 200 ps of run 1.

Figure 3 indicates dynamics on two very different time scales. Fast motions within potential wells reach their equilibrium distribution before a significant number of conformational transitions occur. Motion on two different time scales is also characteristic of the correlation function decays discussed in section IV.

Can the torsion librational motions shown in Figure 3 quantitatively account for the C−H vector correlation function decay at short times? The inset of Figure 2b shows that the initial drop in the correlation function is mostly finished in less than 1 ps. Figure 3 shows that $P(|\Delta\phi|)$ evolves very slowly after about 0.3 ps. Substitution of $\Delta\phi(t)$ for $\theta(t)$ in eq 3 yields an average $CF(t=0.3$ ps) of 0.84 for torsions da, ab, and cd. In Figure 2a, the average value of $CF(t=0.3$ ps) is 0.83 for C−H bond vectors a, c, and d. Thus the short-time decay of the correlation function is due substantially to librational motion in torsional potential wells.

Conformational Transitions. In order to discuss conformational dynamics in polymers, one must choose a particular definition of a conformational transition. We define a conformational transition as the change of a torsional angle from the minimum of one potential well to the minimum of an adjacent well.[38] We use the *last* time the torsion crossed the barrier peak on the way to the second well bottom as the transition time τ_{trans}.[13] There are other reasonable ways to define a conformational transition,[5,6] but we believe that a reanalysis of our results using one of these would leave our conclusions unchanged.

Polyisoprene has three different torsions per repeat unit and the conformational transitions of each had distinct characteristics in our simulation. We counted 609 total conformational transitions in the central 25 repeat units during the 990 ps of run 1. Of this total, 17% were at an ab torsion, 44% were at a cd torsion, and 39% were at a da torsion. Figure 4 is a map[6] of where conformational transitions occurred for the central 25 repeat units (75 total torsions) during the last 200 ps of the simulation. More conformational transitions occurred for torsions 1−37 than for 38−75 during these 200 ps and during the entire trajectory. Presumably, this behavior would average out in a much longer trajectory. This type of heterogeneity may be representative of what one particular configuration of a real polyisoprene chain might show during a single ns.

Cooperativity in Conformational Transitions: Torsion and Position Coupling. It has long been recognized that conformational transitions along a polymer backbone cannot be completely isolated events.[39,40] In the absence of any cooperativity, a conformational transition would involve moving the tails of the chain rigidly in a large arc through the solvent. Polymers have many internal degrees of freedom which cooperate in order to minimize the spatial displacement accompanying a conformational transition. This cooperativity might involve bond bending, small torsional adjustments nearby the transforming bond, and/or additional conformational transitions. Here we investigate the length scale over which this cooperativity occurs for polyisoprene in dilute solution. How far down the chain do atoms adjust their positions in response to a conformational transition?

We first consider cooperativity with neighboring torsions using a method developed by Adolf and Ediger.[13] Conceptually, we take a snapshot of the atomic positions on a section of the chain just before and just after a triggering conformational transition. By averaging over all the transitions in a trajectory, we determine the average displacements of neighboring torsions which accompany a conformational transition. Mathematically, we calculate

$$\langle|(\phi(\tau_{trans}+\Delta t) - \phi(\tau_{trans}-\Delta t)|\rangle \qquad (6)$$

As above, ϕ represents a torsional coordinate. Typically we calculate the quantity shown for the 20 torsions on each side of the transforming bond and average over all transitions of a given type (ab, cd, or da) which occur in the trajectory.

The results of this torsion coupling analysis ($\Delta t = 0.5$ ps) are shown in Figure 5. Position zero on the abscissa is defined by the triggering conformational transition. Positions to the right and left represent neighboring torsions. For example, for torsion ab in Figure 5, position −1 is a da torsion, +1 is a cd torsion, −2 is a cd torsion, +2 is a da torsion, etc. Note that the double bond (torsion bc) is not included in this analysis. The maximum angular distortion is found at position 0 in each case. Far away on either side of position 0, the baseline presumably represents torsional motion un-

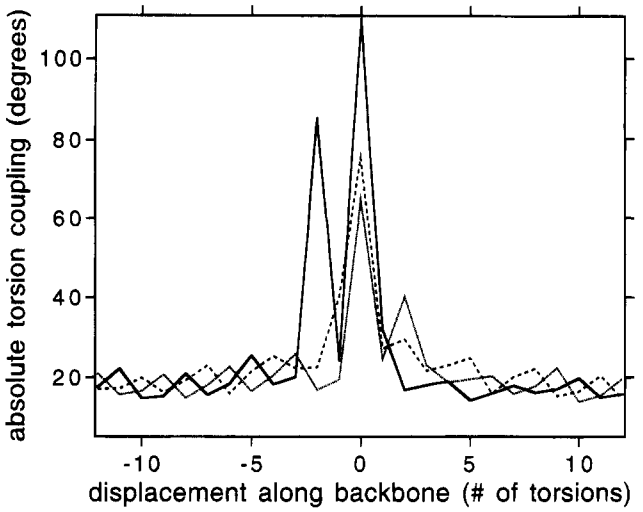

Figure 5. Change in torsional angles accompanying a conformational transition at position zero for the three torsions of polyisoprene (eq 6, Δt = 0.5 ps). Labeling scheme is the same as in Figure 1. Most of the angular adjustments occur within one repeat unit of the transforming bond.

coupled to the triggering conformational transition. Every third torsion in the baseline shows more displacement than its neighbors; this is because the cd torsional potential is "looser" (see Figure 1) than the other two and allows on average more rotational motion in the same amount of time ($2\Delta t$). The baseline in Figure 5 is reached quite rapidly. The region of enhanced displacement appears to be limited to 3 or 4 torsions, or about one repeat unit. This result is entirely consistent with the results of the Brownian dynamics simulation of Adolf and Ediger.[13]

The large secondary peaks in Figure 5 (at position −1 for torsion da, +2 for torsion cd, and especially at position −2 for torsion ab) indicate the torsional motions most strongly coupled to the conformational transition. Sometimes a second conformational transition occurs at these sites, although this happens less than 50% of the time (see below). The location of these peaks indicates that the majority of the cooperativity observed is localized to the flexible regions between double bonds in polyisoprene. The $-CH{=}C(CH_3)-$ groups are essentially rigid and seem to serve as anchor points.

It is possible that some cooperativity is hidden under the oscillating baseline of Figure 5. In order to investigate this and to build a more detailed picture of torsion coupling, expression 6 was modified as suggested in ref 41. Instead of calculating the average of the *absolute value* of the angular displacements of torsions neighboring a conformational transition, we calculated the average displacement *in the same direction* as the triggering transition.

$$\langle A(\Delta\phi)|(\phi(\tau_{trans}+\Delta t) - \phi(\tau_{trans}-\Delta t))|\rangle \qquad (7)$$

Here $A(\Delta\phi)$ is chosen to be ± 1 in order to accomplish this. For example, if a torsion at position 1 rotates in the same sense as the conformational transition (at position 0), it counts positively toward the average; if it rotates in the opposite sense, it counts negatively.

The main part of Figure 6 shows expression 7 for run 1. The baseline goes to zero because distant torsions do not care whether they move with or against the triggering conformational transition. As in Figure 5, the region of enhanced distortion is about one repeat unit for each type of torsion. The large negative peaks

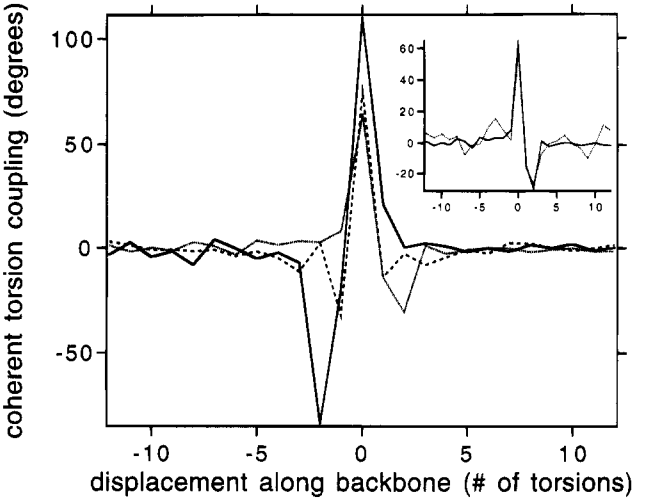

Figure 6. Change in torsional angles accompanying a conformational transition at position zero (eq 7, Δt = 0.5 ps). Change relative to the rotation sense of the transforming bond is shown for the three torsions of polyisoprene (labeling is the same as in Figure 1). Most of the angular adjustments occur within one repeat unit of the transforming bond. The inset shows the same quantity for torsion cd calculated from two trajectories with different starting configurations: run 1 (thick line); run 3 (thin line).

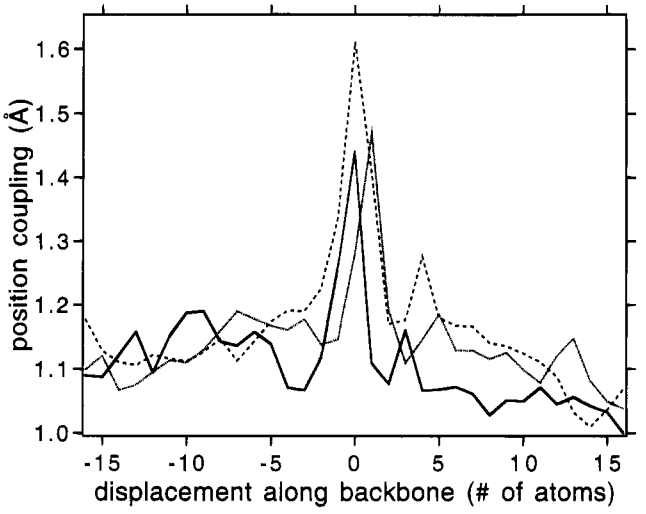

Figure 7. Distortion of atomic positions accompanying a conformational transition for the three torsions of polyisoprene (eq 8, Δt = 0.5 ps). Labeling scheme is the same as in Figure 1. The conformational transition occurs between atoms 0 and 1. The region of enhanced distortion is limited to 1−2 repeat units.

indicate substantial counterrotation cooperativity,[40] which appears to predominate over corotation. The inset to Figure 6 compares the coherent torsion coupling for the cd torsion in runs 1 and 3. The results from run 3 are quite similar to those of run 1 (considering the much poorer statistics of the shorter run) even though a different chain configuration was used and the calculated τ_c values were longer by almost a factor of 3.

It is also possible to calculate the average changes in atomic positions accompanying a conformational transition:[13]

$$\langle|\vec{r}(\tau_{trans}+\Delta t) - \vec{r}(\tau_{trans}-\Delta t)|\rangle \qquad (8)$$

This analysis for run 1 is shown in Figure 7. The site of the triggering transition defines backbone atoms zero and one on the abscissa. For example, for torsion ab,

position 0 is atom a, position 1 is atom b, position 2 is atom c, position −1 is atom d, etc. We see maximum displacement at position 0 or 1. For each torsion, the atom which displays the most mobility is that farthest from the double bond, or more specifically farthest from atom b, which carries the methyl group. This again supports the view of the double bond functioning to localize cooperativity. Consistent with Brownian dynamics simulations on polyisoprene,[13] the region of enhanced distortion is on the order of one or possibly two repeat units (4 backbone atoms per repeat unit). The unevenness of the baseline is related to the dynamic heterogeneity mentioned above. The left half of the chain moved faster on average than the right half, and so we are likely to see more motion to the left of a given conformational transition than to the right. An uneven baseline would also be evident in Figure 5 if the abscissa were extended further from the triggering transition.

We have performed the analyses shown in Figures 5−7 for a number of different values of Δt in expressions 6−8. We chose a short Δt (0.5 ps) in order to minimize baseline noise. The torsion coupling plots in Figures 5 and 6 are qualitatively insensitive to the choice of $\Delta t <$ 50 ps. The position coupling plots lose their features under the rising baseline if $\Delta t \geq 5$ ps. For Δt between 0.5 and 5 ps, the position coupling plots may exhibit a region of enhanced motion wider than 2 repeat units; we cannot be certain of this given that the results are noisy.

Adolf and Ediger in their Brownian dynamics simulation also investigated the coupling of neighboring bond stretching and bending degrees of freedom to conformational transitions.[13] Bond bending was found to be coupled to conformational transitions over a slightly larger length scale than were torsions for short Δts, while bond stretching displayed no detectable coupling for any value of Δt. We speculate that similar results would be obtained if our molecular dynamics trajectories were similarly analyzed.

Cooperativity in Conformational Transitions: Cooperative Transition Pairs. Often cooperativity in conformational transitions has been addressed in terms of cooperative transition pairs.[5,6,13,38,42] While we believe that the torsion and position coupling analysis discussed above is a more general and useful approach to the issue of cooperativity, we have also analyzed our simulations in terms of cooperative transition pairs.

When calculating the fraction of transitions which occur as cooperative transition pairs, one needs to consider both time and space cutoffs. That is, when looking at a map like Figure 4, one must define what constitutes a cooperative pair. We have used two methods to analyze our simulations. The first method limits cooperativity through second neighbors and is similar to the approach taken to refs 13, 31, and 42. We will also describe a more general approach and state the results. Both calculations were limited by the relatively small number of conformational transitions in our trajectory.

In the first approach, the time scale of cooperativity was determined using Brownian dynamics calculations on polyisoprene as reference. Adolf and Ediger[13] observed an average transition time of 165 ps and used a cutoff of 3.0 ps. Since we observed an average transition time of 120 ps, we scaled the cutoff time to 2.2 ps. This is admittedly a crude approximation; however, the small number of transitions observed in our simulation would make it difficult to establish this cutoff directly from the curvature of a hazard plot of first passage times. Using this method, we calculated that 20% of all conformational transitions were cooperative with their first neighbors and 25% with their second neighbors. This result is in general agreement with the Brownian dynamics simulation,[13] which also found that less than half of transitions were involved in cooperative transition pairs.[43] It should be noted that these percentages include random events which coincidentally occur within the specified time and space cutoffs.[31]

The second method of analyzing cooperative transition pairs was motivated by the possibility of cooperativity beyond second neighbors and on longer time scales than considered in the previous analysis. In other words, while looking at a map like Figure 4, we wanted to cast our net wide enough in the spatial and temporal dimensions to pick up all cooperative events. However, we expect that many of the events occurring in a large window occur independently of a triggering conformational transition. These random events need to be quantified in order to determine the fraction of events which are truly cooperative.

The analysis proceeds in two interrelated parts. The first task is to establish length and time scales of cooperativity which will encompass all cooperative events. This part is described below. The second involves accounting for random events which occur in the above space and time window and calculating the fraction of cooperative transitions. We present a statistical method for accomplishing this in the Appendix and state the results in the text below.

To establish the length scale of cooperativity, we calculated the fraction of apparently cooperative events for 1st through 12th neighbors of conformational transitions. Calculations were done for each type of torsion using various cutoff times Δt.[44] These fractions represent the probability that a conformational transition at position j is accomplished by a conformational transition at position k within $\pm\Delta t$ and are stored in 3×25 matrices (3 types of torsions × 25 neighboring positions along the chain). From these fractions, we subtracted an estimate of the fractions of random events (see Appendix) to obtain the fraction of cooperative transitions for each neighbor of each type of torsion. Figure 8 plots these values, which we averaged (for simplicity) in both directions along the chain and over all three types of torsions. As expected, far from the conformational transition at position 0, the probability of a cooperative event goes to zero. This happens somewhat between 6 and 10 torsions away from the triggering transition, so we chose 10th neighbors to be the spatial cutoff.

To pick the best value for the time cutoff Δt, we calculated the areas under the various curves through 10th neighbors. This quantity (inset to Figure 8) appears to reach its asymptotic limit in about 10 ps, indicating that cooperative events appear to finish accumulating by this time. The Appendix describes how the cooperative fraction of conformational transitions is then calculated. We found that the transitions were 15−21% cooperative through first neighbors, 36−43% cooperative through second neighbors, 55−65% cooperative through fourth neighbors, and 60−70% cooperative if up to sixth neighbors were included. A few more percent was added considering through tenth neighbors.

Figure 4 indicates that many conformational transitions are closely followed by another transition at the

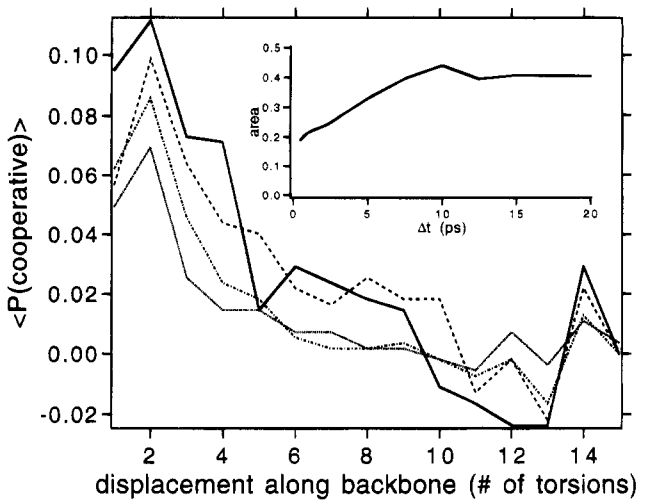

Figure 8. Fraction of cooperative transitions (after subtracting random events) found to occur in neighboring torsions, averaged over all three types of torsions and both chain directions. Values of Δt are 0.5 ps (thin line), 2.5 (- • -), 10 (thick line), and 20 (- - -). Cooperative transitions extend to about 10th neighbors. The inset shows the area under these curves plotted vs Δt. Cooperative events stop accumulating after about 10 ps.

same torsion. We calculated that nearly one-third of all conformational transitions show this "zero-neighbor" coupling, after subtracting out random events. In most cases, this probably involves a quick return to the initial position. If "zero-neighbor" coupling is included in the analysis above, we calculate that at least 73% of all conformational transitions through sixth neighbors are involved in cooperative transition pairs.[45]

Many different types of cooperative transition events were found in our analysis. Two particular types were more prominent than others. When a conformational transition occurred at torsion cd it was sometimes closely followed by a transition two bonds to the right at torsion ab. Transitions at torsion ab were sometimes closely followed by a transition two bonds to the left at torsion cd. Together these cooperative transition pairs which occur between double bonds account for about 17% of all transitions. As discussed in the paragraph above, about 30% of all transitions are involved in cooperative zero-neighbor events. Other than these two types of events, no other type of cooperative transition pair accounted for more than a few percent of the events observed.

VI. Concluding Remarks

This simulation agrees quite favorably with experiment and with a previous Brownian dynamics simulation, suggesting that the simulated dynamics are a fair representation of reality. Very fast librational motion can substantially explain the initial drop in the polymer backbone C–H correlation functions. According to a position and torsion coupling analysis, the region of a polymer which rearranges as a result of a conformational transition is about one repeat unit. Considering up to second neighbors, most conformational transitions are found to be isolated. An analysis which considered more extended coupling along the chain found that most conformational transitions occur as cooperative transition events.

Although our analysis indicates that a majority of transitions occur in cooperative transition events, many different types of such events were found. If we exclude relatively uninteresting events where a given torsion returns to its starting conformation, the most probable type of cooperative transition pair accounts for only 17% of all transitions; other types account for no more than a few percent of the total. Thus, no simple picture involving only rotational isomeric states can represent cooperativity in polyisoprene. Instead, we suggest that the following view of cooperativity is more useful for this type of polymer. When a conformational transition occurs, many degrees of freedom within 1–2 repeat units adjust in order to localize the distortion of atomic coordinates. Torsional angles are particularly important in this process. A considerable fraction of the time a neighboring torsion adjusts enough to cause a second conformational transition, but this happens in a wide variety of ways. In consequence, the displacements of neighboring torsional angles are more usefully viewed as a continuous process instead of one involving discrete rotational isomeric states. Figures 5–7 show some convenient ways of doing this.

Brownian dynamics,[46] by virtue of its treatment of the solvent as a viscous continuum, is much more efficient than molecular dynamics. In light of the general agreement between Brownian and molecular dynamics simulations for polyisoprene solutions, what is gained by using molecular dynamics to study local polymer motions? Brownian dynamics has difficulty reproducing absolute time scales of motion. The Brownian dynamics algorithm inherently produces dynamics which scale linearly with the solvent viscosity. In contrast, experiments show that the dynamics of many flexible polymers in solution have a sublinear dependence on solvent viscosity.[30] High-frequency motion (like librations) is overdamped in a Brownian dynamics simulation. In spite of these shortcomings, it appears that Brownian dynamics simulations may give an adequate picture of the length scale of cooperativity important in conformational transitions. It is important to note that the present comparison is not definitive as different force fields and molecular structures were used in the two simulation schemes.

The systematic simulation of the local dynamics of a series of polymers promises to enhance our understanding of structure/property relationships. It will be particularly interesting to compare the length scales associated with conformational transitions in different polymers. This length scale may correlate with the glass transition temperature.[46]

Acknowledgment. This work was supported by the National Science Foundation (DMR-9123238). N.E.M. is grateful to the U.S. Department of Education for a fellowship. M.D.E. thanks the Alfred P. Sloan Foundation for fellowship support. The computers used in this work were purchased through a grant from the NSF Chemistry Division (CHE-9007850). We thank Young Hwa Kim and Joel Nelson for performing some preliminary simulations on this system. We also thank an anonymous reviewer for carefully reading the manuscript.

Appendix

We used several different reasonable schemes to generate the fraction of conformational transitions in a given time/space window which are random events (i.e., not correlated with a triggering transition). One method can be described as follows: For every observed conformational transition at torsion i, we generated some number (100 for example) of points randomly on the

time axis of Figure 4 along torsion i. For each of these points, we tallied actual conformational transitions which occurred in a time window $\pm\Delta t$ and were spatially within $i \pm 12$ torsions. These values were stored in 3 $\times$ 25 matrices. From these numbers we were able to calculate the probability that a conformational transition had occurred at each position within $i \pm 12$ *regardless* of whether the window was centered on a conformational transition. We calculated this probability individually for each type of torsion (ab, cd, da) at each neighboring position between $i \pm 12$. This calculation is similar to the one described in the text, except that here we do not trigger from a conformational transition. This method may slightly overestimate the fraction of random events because the calculation can still coincidentally trigger near a conformational transition.

A second method used was similar to the one described above except that we restricted our random points along torsion i to be at least $2\Delta t$ away from any observed conformational transition on torsion i. Here we calculated the probability of conformational transitions occurring at each neighboring position between $i \pm 12$ and within a window $\pm\Delta t$ containing no temporal overlap with any window centered on a real conformational transition on torsion i. This method generated a smaller fraction of random events as it biased sampling toward "slower" parts of the trajectory.

To calculate the fraction of conformational transitions occurring as cooperative events, we considered all possible pairs of conformational transitions. Those that were between 1st and 10th neighbors and within $\Delta t = \pm 10$ ps from each other became candidates for cooperative pairs. A given pair of transitions was considered cooperative if a random number between 0 and 1 was larger than the fraction of random events for that pair. Care was taken not to count the same transition as cooperative more than once. For example, if conformational transition 1 is cooperative with transition 2 and transition 2 is cooperative with transition 3, three (rather than four) transitions were counted as cooperative.

From the above example, one should note that transitions are not just occurring in pairs, but often in more extended clusters which defy simple categorization (hence "cooperative events" rather than "cooperative pairs"). We cycled through all possible pairs of transitions many times and averaged the resulting fractions of cooperative events to improve statistics. The range in the numbers reported in the text results from using different methods to calculate the random events. We believe that the numbers likely represent upper and lower bounds.

References and Notes

(1) Pschorn, U.; Rössler, E.; Sillescu, H.; Kaufmann, S.; Schaefer, D.; Spiess, H. W. *Macromolecules* **1991**, *24*, 398.
(2) Schaefer, D.; Spiess, H. W.; Suter, U. W.; Fleming, W. W. *Macromolecules* **1990**, *23*, 3431.
(3) Kim, E.-G.; Misra, S.; Mattice, W. L. *Macromolecules* **1993**, *26*, 3424.
(4) Roe, R. J. *Adv. Polym. Sci.* **1994**, *116*, 111.
(5) Boyd, R. H.; Gee, R. H.; Jin, H. *J. Chem. Phys.* **1994**, *101*, 788.
(6) Zuniga, I.; Bahar, I.; Dodge, R.; Mattice, W. *J. Chem. Phys.* **1991**, *95*, 5348.
(7) One previous example is: Depner, M.; Schurmann, B. L.; Auriemma, F. *Mol. Phys.* **1991**, *74*, 715.
(8) Gisser, D. J.; Glowinkowski, S.; Ediger, M. D. *Macromolecules* **1991**, *24*, 4270.
(9) Glowinkowski, S.; Gisser, D. J.; Ediger, M. D. *Macromolecules* **1990**, *23*, 3520.
(10) Dejean de la Batie, R.; Lauprêtre, F.; Monnerie, L. *Macromolecules* **1989**, *22*, 122.
(11) English, A. D. *Macromolecules* **1985**, *18*, 178.
(12) Schaefer, J. *Macromolecules* **1973**, *6*, 882.
(13) Adolf, D. B.; Ediger, M. D. *Macromolecules* **1991**, *24*, 5834.
(14) Biosym Technologies Inc., San Diego, CA.
(15) (a) Maple, J. R.; Dinur, U.; Hagler, A. T. *Proc. Natl. Acad. Sci. U.S.A.* **1988**, *85*, 5350. (b) Maple, J. R.; Thacher, T. S.; Dinur, U.; Hagler, A. T. *Chem. Des. Automat. News* **1990**, *5* (9), 5.
(16) Moe, N. E. Ph.D. Thesis, University of Wisconsin, in preparation. This reference provides a tabulation of the parameters used in the simulations reported here.
(17) Heatley, F. *Prog. Nucl. Magn. Reson. Spectrosc.* **1979**, *13*, 47.
(18) Jones, A. A., unpublished.
(19) Brandrup, J.; Immergut, E. H. *Polymer Handbook, 2nd ed.*; Wiley: New York, 1975.
(20) We assumed that a 35-mer in a good solvent is not significantly expanded above Θ-dimensions and that the limiting value of the characteristic ratio C_∞ is applicable.
(21) Adachi, K.; Imanishi, Y.; Kotaka, T. *J. Chem. Soc., Faraday Trans. 1* **1989**, *85*, 1065.
(22) Baur, D. R.; Alms, G. R.; Brauman, J. I.; Pecora, R. J. *J. Chem. Phys.* **1974**, *61*, 2255.
(23) Hamza, M. A.; Serratice, G.; Stebe, M.-J.; Delpeuch, J.-J. *Adv. Mol. Relax. Interact. Proc.* **1981**, *20*, 199.
(24) Pickup, S.; Blum, F. D. *Macromolecules* **1989**, *22*, 3961.
(25) Gisser, D. J.; Ediger, M. D. *J. Phys. Chem.* **1993**, *97*, 10818.
(26) von Meerwall, E. D.; Johnson, B. S., unpublished results.
(27) Linse, P. *J. Am. Chem. Soc.* **1984**, *106*, 5425.
(28) Glowinkowski, S., unpublished results.
(29) See ref 10. This result has been questioned by: Rossler, E.; Eiermann, P. *J. Chem. Phys.* **1994**, *100*, 5237.
(30) Zhu, W.; Gisser, D. J.; Ediger, M. D. *J. Polym. Sci., Polym. Phys. Ed.* **1994**, *32*, 2251.
(31) Weber, T. A.; Helfand, E. *J. Phys. Chem.* **1983**, *87*, 2881.
(32) Smith, G. D.; Yoon, D. Y.; Zhu, W.; Ediger, M. D. *Macromolecules* **1994**, *27*, 5563.
(33) Hall, C. K.; Helfand, E. *J. Chem. Phys.* **1982**, *77*, 3275.
(34) Strictly speaking, Hall and Helfand calculated the conformational correlation function and not an orientation autocorrelation function. However, we will follow several subsequent workers who have tested the Hall–Helfand model against orientation autocorrelation functions.
(35) Jones, A. A.; Stockmayer, W. H. *J. Polym. Sci., Polym. Phys. Ed.* **1977**, *15*, 847.
(36) Bendler, J. T.; Yaris, R. *Macromolecules* **1978**, *11*, 650.
(37) Reference 10 modified the Hall–Helfand function to account for librations.
(38) Helfand, E.; Wasserman, Z. R.; Weber, T. A. *Macromolecules* **1980**, *13*, 526.
(39) Schatzki, T. F. *J. Polym. Sci.* **1962**, *57*, 496.
(40) Helfand, E. *Science* **1984**, *226*, 647.
(41) Bahar, I.; Erman, B.; Monnerie, L. *Macromolecules* **1992**, *25*, 6315.
(42) Baysal, C.; Erman, B.; Bahar, I. *Macromolecules* **1994**, *27*, 3650.
(43) We looked both forward and backward in time from the triggering transition in order to calculate the fraction of cooperative transition pairs. This approach was used since any given transition could either initiate a cooperative event or terminate it. Since ref 13 looked only forward in time, the numbers reported there must be doubled in order to compare to the present results. After doubling, the Brownian dynamics simulations indicate that 40% of all transitions occur as cooperative transition pairs (through second neighbors).
(44) Cooperative transition pairs were searched for both forward and backward in time.
(45) Substantial zero-neighbor coupling was found in a recent MD simulation of bulk polyethylene.[5]
(46) Ediger, M. D.; Adolf, D. B. *Adv. Polym. Sci.* **1994**, *116*, 73.

MA9450849